FLEXURAL EDGE WAVES ALONG FREE AND IMMERSED ELASTIC WAVEGUIDES

Jacques R. Chamuel
Sonoquest Advanced Ultrasonics Research
P.O. Box 81153, Wellesley Hills, MA 02181-0001

INTRODUCTION

A collection of fundamental experimental results on edge waves propagating along the edge of free and immersed elastic wedges and plates were presented at the Special Session entitled "Long-Range NDE Using Guided Waves/Extended Overviews" chaired by Professor S. Rokhlin. This paper summarizes the experimental results discussed on the effect of wedge apex truncation and water loading on the phase velocity of the slowest antisymmetric flexural wedge mode. The remaining results that were presented on plate edge flexural waves and edge waves along elastic wedges with range-dependent apex angle are described elsewhere [1-4].

The following paper consists of two sections. The first section presents quantitative experimental results characterizing the dispersion of antisymmetric edge waves propagating along the apex of a truncated elastic wedge using contactless electromagnetic acoustic transduction [5]. The experimental results are compared with theoretical calculations by McKenna et al. [6] and other anomalous experimental results observed by Jia et al. [7-8] based on laser ultrasonics.

The second section of the paper presents the first available quantitative experimental results demonstrating: a) the extremely low velocity of flexural edge waves along sharp wedges with apex angle less than 15°, and b) the effect of water loading on drastically reducing the wedge wave velocity and changing the velocity profile from concave to convex when plotted as function of wedge angle as predicted by Krylov [9]. The experimental results demonstrate that unlike the immersed plate case, water loading is more pronounced as the wedge angle is decreased.

Fundamental understanding of wedge waves is essential for nondestructive testing, underwater acoustics, acoustoelectronics, seismology, acoustic imaging, noise control, and sensors. Wedge waves can propagate for example along edges of propeller blades, finite crystals, cutting tools, mountains, Arctic ice, cracks, airfoils, underwater fins, and ridges. Flexural edge waves have been used to measure linear and angular displacement, liquid level, and cutting edge sharpness [10]. The author hypothesises that wedge waves can trigger avalanches of snow, ice, earth or rock down a precipice or mountain side. Krylov [9] proposed using wedge waves for wave-like propulsion of small underwater vehicles.

DISPERSION OF EDGE WAVE ALONG TRUNCATED ELASTIC WEDGE

Edge waves propagating along the apex of an elastic wedge were discovered in 1972 independently by Lagasse [11] and by Maradudin et al. [12] . These wedge waves are not to be confused with flexural edge waves propagating along the edge of a plate [13]. The results presented in this section are limited to the study of antisymmetric wedge waves.

Review of Progress in Quantitative Nondestructive Evaluation, Vol 16
Edited by D.O. Thompson and D.E. Chimenti, Plenum Press, New York, 1997

Lagasse obtained an empirical relationship between the velocity V of antisymmetric wedge modes and wedge angle Θ:

$$V = V_R \sin(n\Theta), \quad n = 1, 2, 3, \ldots, \quad n\Theta < 90° \qquad (1)$$

where V_R is the Rayleigh wave velocity on a half-space, and n is an integer representing the mode order. The antisymmetric wedge modes are nondispersive and the number of existing modes depends on Θ. As the wedge apex angle decreases, the number of antisymmetric wedge modes increases. Experimental results using broadband pulses were presented in References [1- 5]. Quantitative studies [2] revealed that a more accurate wedge mode velocity was obtained when V_R in the above equation was replaced with the edge Rayleigh wave velocity V_{RE} existing along the edge of an elastic quarter-space (Θ = 90°). McKenna et al. [6] obtained theoretical and numerical results demonstrating the influence of apex truncation on the dispersion of antisymmetric wedge modes. The purpose of this section is to present high precision quantitative experimental results characterizing the dispersion of antisymmetric wedge waves propagating along wedges with truncated apex using contactless electromagnetic acoustic detection [4-5].

Experimental Setup

Aluminum 6061 was used to fabricate a sharp wedge with an apex angle Θ = 26.7°. The wedge dimensions were chosen to separate in time any wave reflections from the surfaces and corners of the wedge base and sides. Ultrasonic wedge waves were generated with a 1.5 mm diameter compressional piezoelectric transducer positioned to excite flexural antisymmetric wedge modes. Specially designed contactless broadband electromagnetic acoustic transducers were used to detect the wedge waves propagating along the apex. The received signal was displayed on a digital oscilloscope (FIG. 1). Waveform and dispersion data were obtained from the initially sharp wedge (3 μm apex) representing the "ideal" wedge. The apex was then truncated successively in steps, and the corresponding dispersion results were recorded.

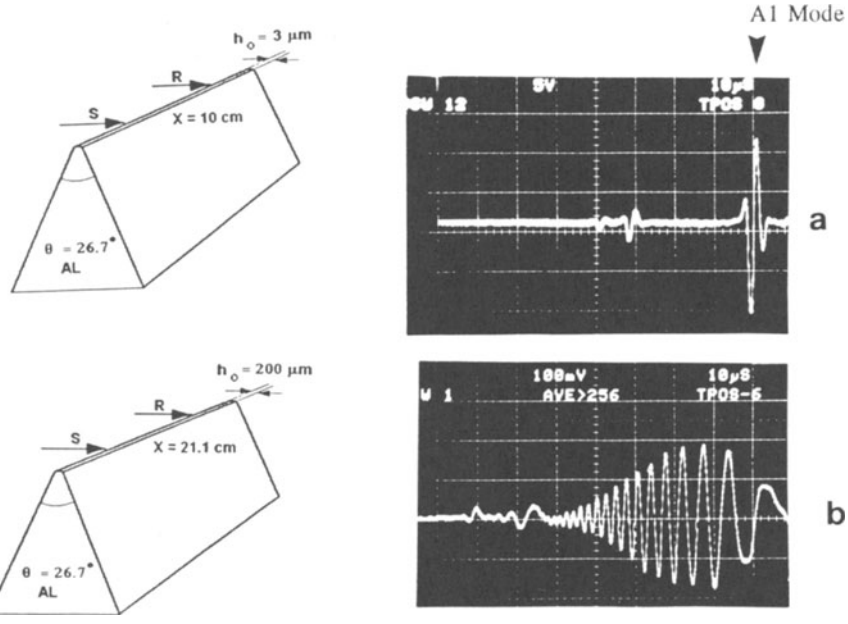

Fig. 1. Experimental setup configuration and waveform of antisymmetric wedge waves along apex of aluminum wedge with apex angle Θ = 26.7°. Top: sharp apex (h_o = 3 μm). Bottom: truncated wedge (h_o = 200 μm).

Results

FIG. 1 shows waveforms of the antisymmetric flexural wedge modes obtained with the source excited with a single broadband pulse. The received waveform from the sharp wedge (h_o = 3 μm) is displayed in FIG. 1(a). Three practically nondispersed pulses are received representing the three allowed modes for the 26.7° wedge. The slowest mode is labelled as the A1 mode. The distance X between source and receiver is 10 cm. A highly dispersive wavetrain is produced by the truncated wedge with h_o = 200 μm (FIG. 1(b)). The single broadband pulse is transformed into this highly dispersive wavetrain.

Phase velocity dispersion plots are generated from gated sinusoidal signals (30-800 KHz). Wavelength measurements are averaged over 10-20 wavelengths. FIG. 2 shows the measured dispersion of antisymmetric wedge waves obtained from the 26.7° aluminum wedge truncated with h_o = 30, 88, 140, and 200 μm. The ratio of truncated wedge phase velocity to the "ideal" sharp wedge velocity is plotted as a function of frequency. The velocity of the high frequency components increases as the wedge truncation h_o is increased. The repeatability of the velocity data points is better than 10^{-4} up to about 500 kHz. Above 500 kHz, the signal-to-noise ratio drops and the accuracy of the data points decreases.

The experimental results on the effect of apex truncation on the dispersion of the slowest antisymmetric flexural wedge mode are compared in Fig. 3 with the theoretical predictions by McKenna et al. [6]. The ratio $V_{truncated}/V_{sharp}$ is plotted as a function of $X_o k$ as presented in Reference [6], where k is the wavenumber and X_o is the vertical distance from the sharp wedge apex to the truncated wedge apex. The experimental results gathered with the contactless electromagnetic acoustic transducer compare favorably with the theoretical calculations based on thin plate approximations. The anomalous laser ultrasonics experimental data described in Reference [7] with Θ = 30° are also replotted as function of $X_o k$ in FIG. 3 for comparison.

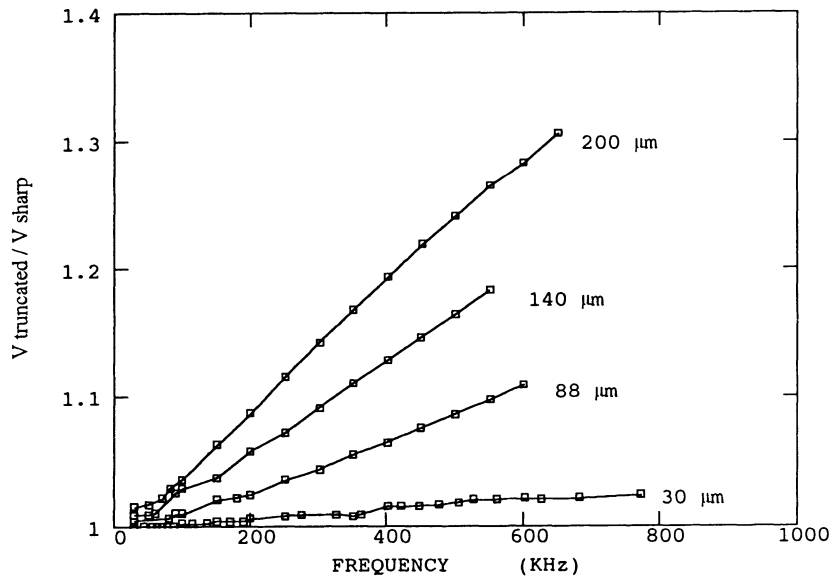

Fig. 2. Dispersion of slowest antisymmetric edge wave from truncated aluminum wedge for different values of h_o (30, 88, 140, and 200 μm). Ratio of A1 wedge mode (phase velocity of truncated wedge) / (phase velocity of sharp wedge) plotted as a function of frequency in KHz.

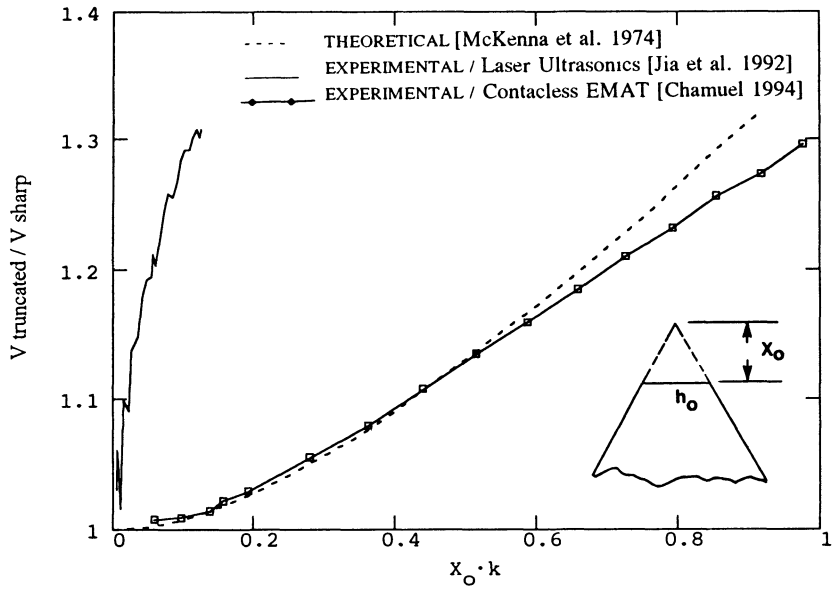

Fig. 3. Experimental results on the effect of apex truncation on the dispersion of the slowest antisymmetric flexural wedge mode compared with the theoretical results of McKenna et al. [6]. The anomalous laser ultrasonics experimental data with $\Theta = 30°$ from Reference [8] are also plotted.

FREE AND IMMERSED SMALL-ANGLE ELASTIC WEDGE

According to Lagasse's empirical equation (1), the flexural wedge wave velocity decreases as the wedge angle Θ is decreased. The shape of the phase velocity curve is convex when plotted as a function of wedge angle similar to the classic flexural wave dispersion curve for thin plates when plotted vs frequency. Krylov [9] modified the thin plate theory to obtain a theoretical expression for the immersed wedge with small apex angle. For immersed small-angle wedges, Krylov [9] predicted that the wedge wave velocity profile is concave. Using Krylov's equation and the elastic properties of Plexiglas and water, the phase velocity of the A1 mode for a free and an immersed small-angle Plexiglas wedge was plotted as a function of wedge angle (FIG. 4). One observes that water loading not only decreases the wedge wave velocity but also changes the characteristics of the curve from near-linear to concave for wedge angles up to 15°.

Quantitative experimental results are presented below demonstrating the extremely low velocity of flexural edge waves along sharp wedges with apex angle less than 15°, and revealing the effect of water loading on reducing the wedge wave velocity and changing the velocity profile to concave when plotted as a function of Θ.

Experimental Setup

The experimental setup is identical to the one mentioned in the previous section except for the wedge models and the receiver transducer. 1.5 mm diameter broadband piezoelectric transducers are used to generate and detect the edge waves.

In order to obtain accurate results, experiments were conducted on one Plexiglas wedge that was remachined to fabricate other smaller angle wedges possessing precisely the same elastic properties. First, a Plexiglas wedge with apex angle $\Theta = 13°$ was fabricated. Measurements from the first wedge were obtained. The 13° wedge was remachined to fabricate a second

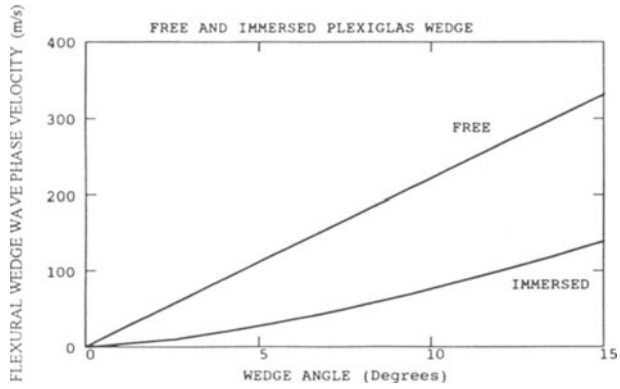

Fig. 4. Comparison of flexural wedge wave velocity (A1 mode) for free and immersed Plexiglas wedge calculated using Krylov's [9] equation.

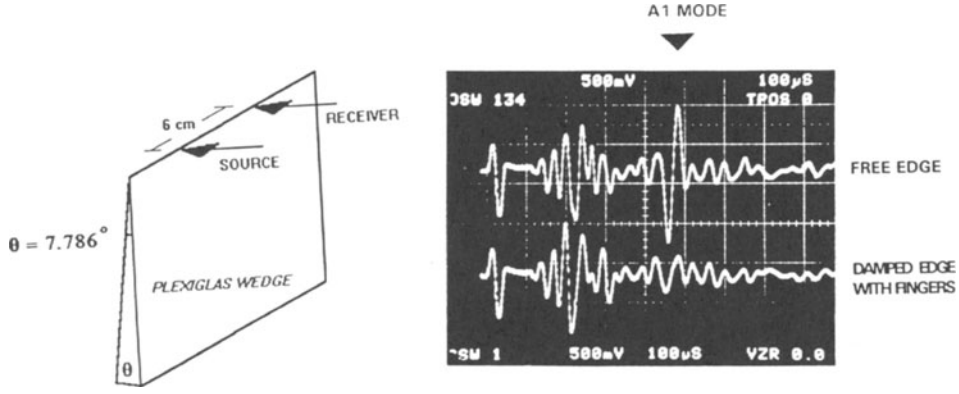

Fig. 5. Extremely slow flexural edge waves observed propagating along edge of free Plexiglas wedge with small apex angle $\Theta = 7.786°$. Top : arrow pointing to A1 mode. Bottom: wedge edge damped with finger tips to attenuate the A1 mode.

Plexiglas wedge with a smaller angle $\Theta = 8.87°$. Measurements were acquired from this second model. The 8.87° wedge was remachined to fabricate a third wedge model with $\Theta = 7.786°$. A final set of measurements were captured from the third wedge.

Results

Several flexural edge modes propagate along the apex of small-angle wedges. The results discussed in this section are focused on the slowest wedge mode (A1 mode). The top oscilloscope trace in FIG. 5 represents the waveform of the received wedge waves obtained from the 7.786° wedge with a 6 cm separation between source and receiver. The bottom trace shows the attenuation of the A1 mode when the wedge apex is damped with the finger tips. The time scale is 100 μs/div. and the A1 mode consists of a single 25 KHz pulse. The edge wave velocity is measured by dividing a change in source/receiver range ΔX by the corresponding change in arrival time Δt of the wedge wave. Fig. 6 compares the waveforms received from the 7.786° wedge with X = 5.23 cm (top trace) and X = 8.23 cm (bottom trace). The A1 mode is delayed by 175 μs as X is increased by 3.00 cm. The measured edge wave velocity is 171 m/s. According to Lagasse's equation (1), the calculated velocity of the A1 mode is 173 m/s.

Repeating the velocity measurements with the Plexiglas wedge immersed in water resulted is slower edge wave velocities. Fig. 7 shows the photograph of two superimposed waveforms obtained from the immersed 7.786° Plexiglas wedge for a ΔX = 2.5mm. The measured corresponding time delay of the A1 mode is 45 μs as demonstrated near the center line of the oscilloscope trace. The measured edge wave velocity for the immersed 7.786° wedge is 55.5 m/s. Using Krylov's equation and the Plexiglas parameters, one obtains a calculated velocity equal to 52 m/s.

The A1 mode velocity measurements obtained from the three different Plexiglas wedge models are plotted in Fig. 8. Theoretical calculations using Krylov's equation [9] are also plotted in FIG. 8. The experimental results confirm Krylov's theoretical predictions and demonstrate that unlike the immersed plate case, water loading is more pronounced as the wedge angle is decreased. FIG. 9 compares the measured ratio of (immersed wedge wave velocity)/(free wedge velocity) as determined from the three wedges. The 13°, 8.87°, and 7.786° wedge angles yielded wedge velocity ratios of 0.385, 0.325, and 0.313 respectively.

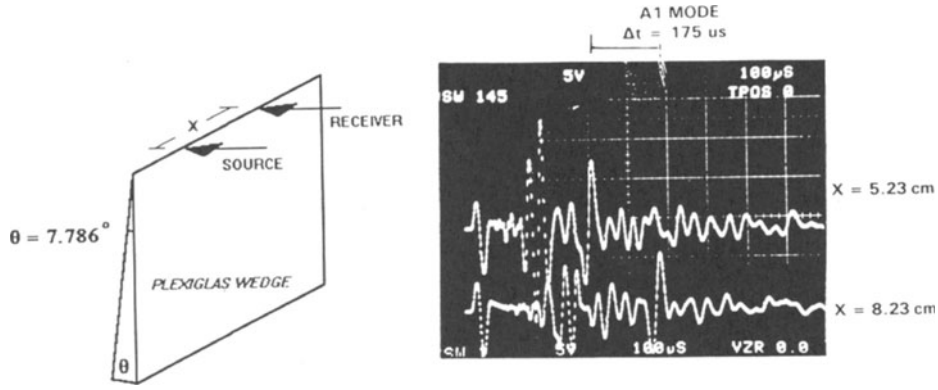

Fig. 6. Measurement of A1 mode phase velocity for small-angle (Θ = 7.786°) Plexiglas wedge in air. A 3.00 cm displacement introduces a 175 μs time delay.

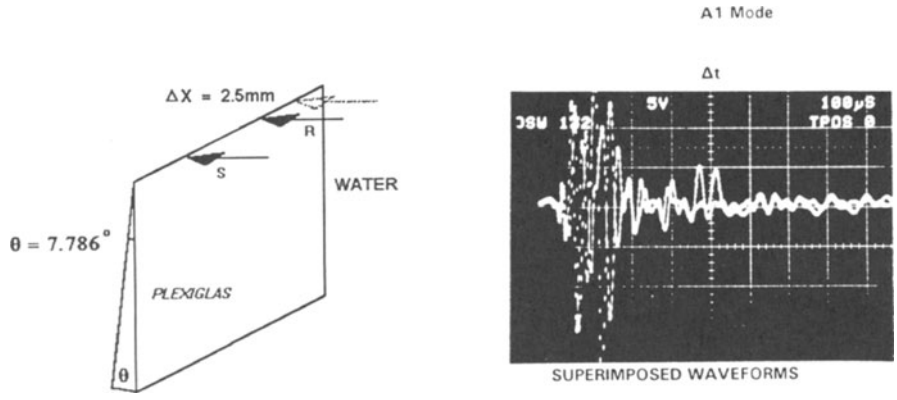

Fig. 7. Measurement of A1 mode phase velocity for immersed small-angle (Θ = 7.786°) Plexiglas wedge in water. A 2.50 mm displacement produces 45.0 μs time delay. Photograph showing superposition of waveforms detected at two ranges X = 2.1911 cm and 2.441 cm.

For the immersed small-angle Plexiglas wedge in water, the author matched Krylov's equation with the following empirical equation between the phase velocity in m/s of the A1 wedge mode and wedge apex angle in degrees:

$$V_w = 2.26\Theta^{1.522} . \quad (2)$$

Other recent numerical and experimental results on large-angle immersed elastic wedge have been reported [14-15].

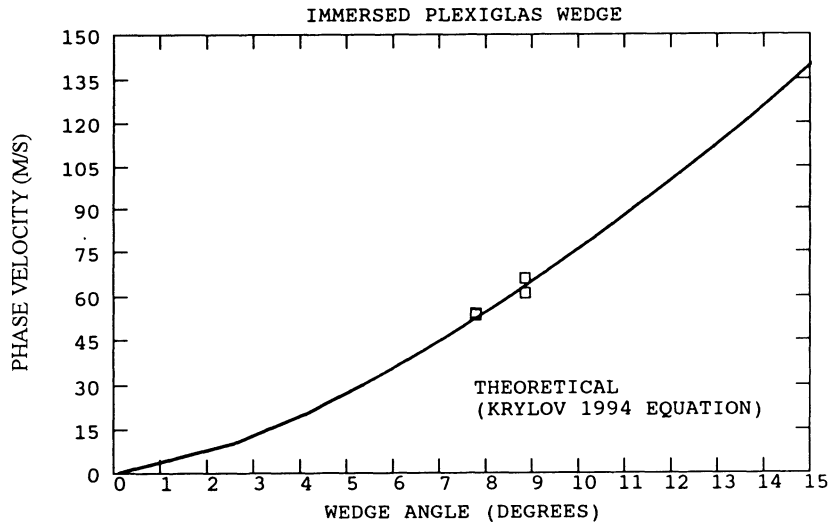

Fig. 8. Water immersed Plexiglas wedge experimental results compared with calculations using Krylov's equation [9]. A1 mode phase velocity in m/s plotted as a function of wedge angle in degrees.

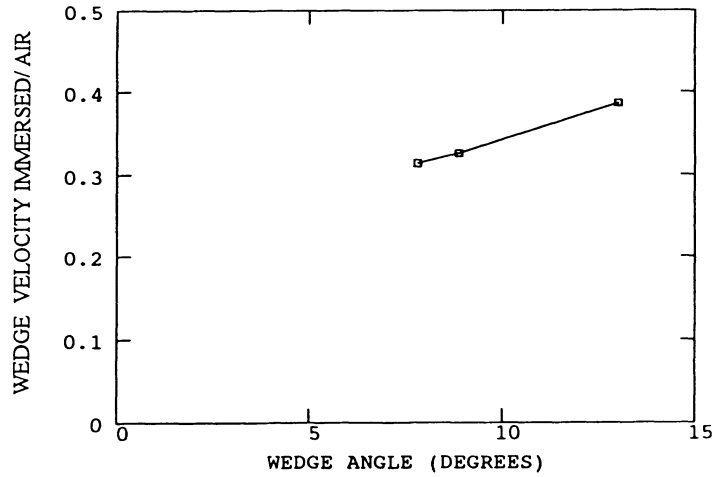

Fig. 9. Plexiglas wedge experimental results. Ratio of (immersed wedge wave velocity)/(free wedge wave velocity) plotted as a function of wedge angle in degrees.

CONCLUSIONS

High precision experimental results were presented characterizing the dispersive behavior of antisymmetric flexural wedge waves propagating along the apex of a truncated elastic wedge. Contactless electromagnetic acoustic detection of antisymmetric wedge waves produced dispersion results generally in agreement with theoretical predictions by McKenna et al. [6].

The paper presented the first quantitative experimental results on free and immersed small-angle elastic wedges. A1 mode phase velocity measurements were plotted as a function of apex angle from immersed small-angle wedges. The experimental results supported the theoretical predictions by Krylov [9] and demonstrated the concave profile of the phase velocity curve when plotted as a function of wedge angle. The extreme slow velocities of wedge waves along small-angle wedges have been demonstrated. For immersed small-angle Plexiglas wedges, velocities as low as 53 m/s were measured. The ratio of (immersed wedge flexural velocity)/(free wedge flexural velocity) decreases as the wedge apex angle is decreased indicating that water loading is more pronounced as the wedge angle is decreased.

REFERENCES

1. J. R. Chamuel, Arctic Acoustics Ultrasonic Modeling Studies, Sonoquest Advanced Ultrasonics Research, National Technical Information Service report accession No. AD-A224165 (March 1990).
2. J. R. Chamuel, "Edge waves along immersed elastic elliptical wedge with range dependent apex angle," Proc. IEEE 1993 Ultrasonics Symp. 313-318 (1993).
3. J. R. Chamuel, Ultrasonic Studies of Transient Seismo-Acoustic Waves in Bounded Liquid/Solid Interfaces, National Technical Information Service report accession No. AD-A243441 (November 1991).
4. J. R. Chamuel, Ultrasonic Studies of Liquid/Solid Seismoacoustic Wave Phenomena, National Technical Information Service report accession No. AD-A289644 (November 1994).
5. J. R. Chamuel, "Contactless characterization of antisymmetric edge wave dispersion along truncated wedge using electromagnetic acoustic transducer," J. Acoust. Soc. Am. 95(5), Pt.2, (1994).
6. J. McKenna, G. D. Boyd, and R. Thurston, "Plate theory solution for guided flexural acoustic waves along tip of a wedge," IEEE Trans. Son. Ultrason. SU-21(3) 178-186 (1974).
7. X. Jia and M. de Billy, "Observation of the dispersion behavior of surface acoustic waves in a wedge waveguide by laser ultrasonics," Appl. Phys. Lett. 61(25) 2970-2972 (1992).
8. X. Jia, D. Auribault, M. de Billy, and G. Quentin, "Laser generated flexural acoustic waves traveling along tip of a wedge," Proceedings IEEE 1993 Ultrasonics Symposium, 637-640 (1993).
9. V. V. Krylov, "Propagation of wedge acoustic waves along wedges imbedded in water," Proc. IEEE 1994 Ultrasonics Symposium, 793-796 (1994).
10. J. R. Chamuel, Patent Applications in progress.
11. P. E. Lagasse, "Analysis of a dispersionfree guide for elastic waves," Electronics Letters 8(15) 372-373 (1972).
12. A. A. Maradudin, R. F. Wallis, D. L. Mills, and R. L. Ballard, "Vibrational edge modes in finite crystals," Physical Rev. B 6(4) 1106-1111 (1972).
13. Y. K. Konenkov, "A Rayleigh-type flexural wave," Soviet Physics Acoust. (6) 122-123 (1960).
14. A. C. Hladky-Hennion, P. Langlet, M. de Billy, "Finite element analysis of the propagation of acoustic waves along the tips of elastic immersed wedges," IACM 3rd Europ. Conf. Underwater Acoustics, Heraklion, Crete, June 1996.
15. M. de Billy, "On the influence of loading on the velocity of guided acoustic waves propagating in linear elastic wedges," J. Acoust. Soc. Am. 100(1), 659-662 (1996).